The Influence of Laminar Separation and Transition on Low Reynolds Number Airfoil Hysteresis

Thomas J. Mueller*
University of Notre Dame, Notre Dame, Indiana

An experimental study of the Lissaman 7769 and Miley M06-13-128 airfoils at low chord Reynolds numbers is presented. Although both airfoils perform well near their design Reynolds number of about 600,000, they each produce a different type of hysteresis loop in the lift and drag forces when operated below chord Reynolds numbers of 300,000. The type of hysteresis loop was found to depend upon the relative location of laminar separation and transition. The influence of disturbance environment and experimental procedure on the low Reynolds number airfoil boundary-layer behavior is also presented.

Nomenclature

c	= airfoil chord, m
C_d	= section profile drag coefficient, $= D/QS$
C_ℓ	= section lift coefficient, $= L/QS$
D	= drag force, N
L	= lift force, N
Q	= dynamic pressure, $= \frac{1}{2}\rho U^2$, N/m^2
R_c	= Reynolds number based on airfoil chord, $= U_\infty \rho c/\mu$
S	= airfoil planform area, m^2
U	= velocity in streamwise direction, m/s
u_{rms}	= root-mean-square of the fluctuating velocity, m/s
α	= angle of attack, deg
μ	= absolute fluid viscosity, kg/m-s
ρ	= density of fluid, kg/m^3

Subscripts

max	= maximum value for variable
min	= minimum value for variable
∞	= freestream value

Introduction

THERE has been an increasing interest in the design and performance of airfoils operating in low Reynolds number flows. This interest has been the result of the desire to obtain better performance for both military and civilian systems. Applications include jet engine compressor and turbine blades and remotely piloted vehicles (RPVs) at high altitudes; and sailplanes, ultra light man-carrying/man-powered aircraft, and mini-RPV's at low altitudes. These systems require efficient airfoil sections in the chord Reynolds number range from about 100,000 to 1,000,000.

Many of the problems that occur at low Reynolds numbers have been known since the early 1900s; however, the first systematic study was accomplished by Schmitz[1] in the early 1940s. This research was originally directed toward model airplanes, but has served as a foundation for many subsequent studies.

Presented as Paper 84-1617 at the AIAA 17th Fluid Dynamics, Plasma Dynamics, and Lasers Conference, Snowmass, Colo., June 25-27, 1984; received July 8, 1984; revision received May 22, 1985.

*Professor, Aerospace and Mechanical Engineering. Associate Fellow AIAA.

Many significant aerodynamic problems occur below chord Reynolds numbers of about 500,000.[2] Although some progress has been made, there are problems requiring more study if further improvements are to be realized. These problems are related to the management of the airfoil boundary layer and the difficulties related to making accurate wind tunnel[3] and free-flight measurements.[4] In relation to the airfoil boundary layer, important areas of concern are the separated regions that occur near the leading and/or trailing edges and transition from laminar to turbulent flow.[2] It is well known that separation and transition are highly sensitive to Reynolds number, pressure gradient, and the disturbance environment.[5] Transition and separation play a critical role in determining the development of the boundary layer which, in turn, affects the overall performance of the airfoil.[2] Hysteresis in the lift and drag forces is relatively common for round-nosed, thick, cambered airfoils at Reynolds numbers below about 300,000. At chord Reynolds numbers somewhere below 300,000 (depending on airfoil geometry), the airfoil boundary layer passes through a critical region. For some airfoils, laminar separation without reattachment may occur due to a strong adverse pressure gradient after the suction peak. For other airfoils, transition occurs soon enough after laminar separation to allow reattachment. At low Reynolds numbers and angles of attack laminar separation with no reattachment is common. The boundary-layer behavior at higher angles of attack is an indicator of the type of hysteresis loop that may occur. If the flow remains separated up to high angles of attack a low $C_{\ell\,\max}$ or counterclockwise hysteresis loop may result. If a separation bubble forms at moderate angles of attack the forces may exhibit a high $C_{\ell\,\max}$ or a clockwise hysteresis loop. Hysteresis is of practical importance because it produces widely different values of $C_{\ell\,\max}$ and $(L/D)_{\max}$. It could also affect the recovery from stall and/or spin flight conditions.

Many of the problems plaguing low Reynolds number research involve the difficulties associated with making accurate wind tunnel models and obtaining reliable data. Because the airfoil boundary layers are sensitive to small disturbances, accurate wind tunnel models and low-disturbance levels in the approaching flow are very important in the evaluation of a given design. Furthermore, because the forces, pressure differences, and velocities are small, a great deal of care must be exercised to obtain accurate and meaningful data.

The primary objective of the present research is to obtain a better understanding of the occurrence and behavior of transition and/or separation, as well as their effect on the overall performance of airfoils, including hysteresis. In addition,

knowledge of the sensitivity of separation and transition to freestream disturbances is important in understanding this complex flow phenomenon and improving analytical techniques of predicting it.

Measurement Techniques

To evaluate and improve existing airfoil design procedures, accurate wind tunnel data are needed. These data include lift, drag, and moment measurements, as well as the determination of the location of transition and separation on two-dimensional airfoil sections and finite wings. The lift force can be determined with acceptable accuracy using a strain-gage balance. If small pressure differences can be measured accurately, then a reasonably accurate lift force can also be obtained by integrating the static pressure distribution around the airfoil. In an atmospheric wind tunnel at low Reynolds numbers (e.g., $R_c = 100{,}000$) this requires accurate pressure difference measurements below 10 mm of water. Since airfoil drag forces are at least an order of magnitude smaller than the lift forces, they are much more difficult to measure accurately when tests are conducted at low R_c. To measure these very small drag forces (e.g., 0.012 N for a 250 mm chord, 420 mm span airfoil section at $R_c = 100{,}000$), a very sensitive, specially designed strain-gage balance arrangement with high signal-to-noise ratio and minimal electronic drift is needed. A balance system of this type is within the state-of-the-art and has been developed at the University of Notre Dame. The major difficulty with this technique is the determination of interference effects between the airfoil and the side plates.[3] This interference is the result of flow separation and the formation of a corner vortex. At low Reynolds numbers (i.e., $R_c < 100{,}000$), the region affected by side-plate interference may be as large as 5% of the span (10% of the span if side plates are on both ends of the airfoil). As the Reynolds number increases, this region of three-dimensional flow decreases in size and effect. As a result of this three-dimensional corner flow region near the ends of the airfoil, the measured drag forces were found to be higher than for the infinite span airfoil. At $R_c = 60{,}000$, the minimum drag coefficient was about 15% higher. This difference decreased as R_c increased—to about 10% at $R_c = 300{,}000$.[3]

Disturbance Environment

The disturbance environment present in the test section of a low-speed wind tunnel is usually determined by freestream turbulence, acoustic phenomena, and mechanical vibrations. The freestream turbulence level depends on the history of the flow in the settling chamber, flow straighteners or screens, and inlet leading to the test section. Acoustic phenomena are related to the noise emitted from turbulent boundary layers on the side walls, unsteady separated flow regions, and the wind tunnel fan and its associated drive system. Mechanical vibrations may be caused by rigid coupling of the fan and drive system to the wind tunnel, as well as by the unsteady wakes of probe and model supports. Although these factors which determine the disturbance environment may be reduced and controlled, they cannot be eliminated completely. It is apparent that, in general, each wind tunnel has a different disturbance environment which is a function of its design and method of fabrication. Therefore, it is not surprising that similar experiments on the same geometry model at low Reynolds numbers often produce results that differ from one wind tunnel to the next.

Results of acoustic and turbulence measurements in the University of Notre Dame low-speed wind tunnels (shown in Fig. 1) indicated that the experimental environment was a complex function of many variables. In the standard configuration, Fig. 1, turbulence intensities measured with a hot-wire anemometer varied from 0.07 to 0.15% over the velocity range from 9 to 31 m/s as shown in Fig. 2. The disturbance environment could be increased artificially by placing a screen at the beginning of the test section or a flow restrictor at the end of the test section and increasing the fan speed as indicated in Fig. 3.[5]

There was a noticeable increase in disturbance intensity at a velocity of 12 m/s. This corresponds to a fan rpm of approximately 460. At this fan rpm there was significant pulsating of the fan blades as the belt drive from the motor appeared to slip at this setting. The pulsating of the fan was accompanied by a slight squeaking of the belts. When a flow restrictor was introduced, the turbulence intensities in the section were increased significantly. The turbulence intensity at idle speed (i.e., 298 rpm) increased from 0.07 to 0.16% when one or two flow restrictors were used (see Fig. 2). The u_{rms} does not decrease as much as the freestream velocity U_∞, which causes the ratio of u_{rms}/U_∞ to increase. A small part of this proportionally larger u_{rms} value may be due to electronic noise. As

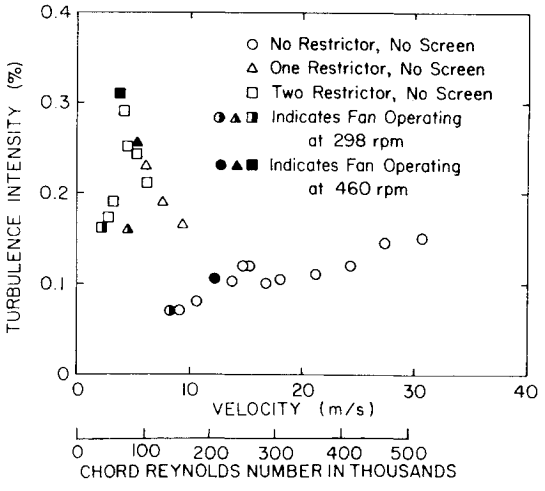

Fig. 2 Turbulence intensity vs test section velocity and chord Reynolds number for 250 mm chord airfoils.

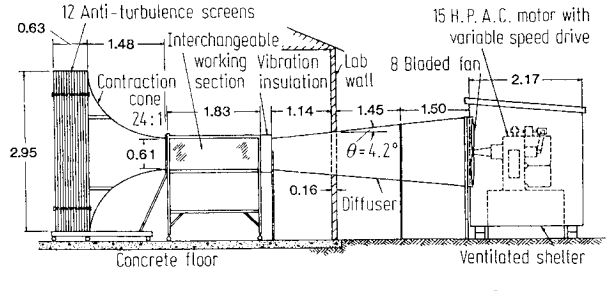

Fig. 1 Low-turbulence subsonic wind tunnel.

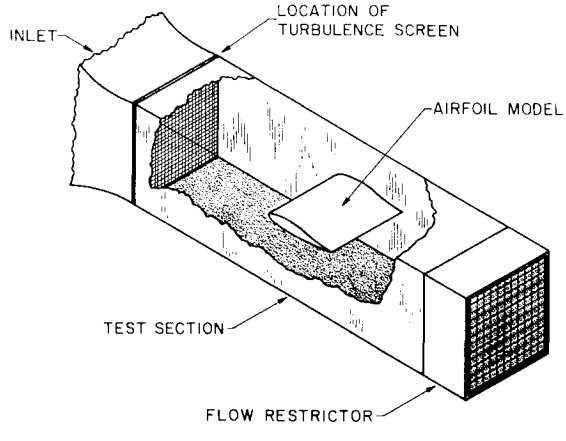

Fig. 3 Test section showing turbulence screen and flow restrictor locations (airfoil side plates not shown).

the mean velocity decreases, the electronic noise maintains the fluctuating signal at a higher level causing an apparent increase in turbulence intensity. With one flow restrictor a large increase in turbulence was observed at 5.5 m/s, while an even larger increase was observed at 3.8 m/s when two flow restrictors were in place. Both of these velocities correspond to a fan rpm of about 460. It may be the increased workload required by the pressure drop through the flow restrictor in conjunction with the pulsating tendency of the fan at this rpm that causes the fan to induce these high turbulence intensities in the test section. Once the 460 rpm region is passed, the turbulence intensities gradually decrease but always remain higher than the no-flow-restrictor case. An important comparison can be made at 9 m/s (approximately a 150,000 chord Reynolds number for the test models), where the tunnel may be operated with no flow restrictor or with one flow restrictor in place. The turbulence intensity increased from 0.07 to 0.16% when one flow restrictor was inserted, changing the test section environment considerably. Introduction of a 7.09-meshes/cm turbulence screen between the test section and tunnel inlet increased the turbulence intensity in the test section to about 0.3%.

Analysis of the sound pressure levels in the test section indicated a different behavior. Sound levels at idle remained constant at approximately 93 dB (referred to 2×10^{-5} N/m^2) regardless of the experimental setup. Introduction of flow restrictors or a turbulence screen did not appear to change the total sound pressure level in the test section for a given fan rpm. However, to achieve the same test section velocity with one flow restrictor in place the fan had to be operated at a higher rpm. When operating at a chord Reynolds number of 150,000 with one flow restrictor in place, a total sound level of 104 dB was measured in the section compared to a much quieter 93 dB at the same velocity with no flow restrictor in use. Special care was taken to visually observe the probes for mechanical vibrations which may have been produced by tunnel vibrations or by the flow over the probe holders. The foam insulation between the test section and tunnel diffuser appeared to successfully damp any mechanical vibrations from the fan motor and no vibration of the hot wire or microphone was observed.

Experimental Apparatus

The wind tunnel with the external strain-gage balance used for the force measurements is shown in Fig. 4. The wind tunnel test section is 610 mm square and 1828 mm in length. A more complete description of the wind tunnel facility is given in Ref. 3. The flow-visualization, pressure, and hot-wire experiments were made in an identical test section, with the model and side plates rotated 90 deg from the force balance configuration, i.e., airfoil horizontal. Smoke-tube and smoke-wire techniques[6] were used to visualize the flow around the airfoil at low Reynolds numbers.

The two airfoil sections used for this study were the Lissaman 7769 and the Miley M06-13-128 shown in Fig. 5. The Lissaman 7769 was designed for a chord Reynolds number of about 600,000 for the Gossamer man-powered aircraft,[7] while the Miley M06-13-128 was designed for about the same chord Reynolds number for the inboard section of a helicopter rotor.[4] Although both airfoils perform very well at their design Reynolds number, they both produce large hysteresis loops when operated at Reynolds numbers below 300,000.

The Lissaman 7769 airfoil model used in the experiments was constructed of wood using two steel end plates machined to the profile of the airfoil. The wood was coated with an epoxy and finished with a smooth surface. The airfoil model had a 437 mm span and a 249 mm chord. Experiments were also performed using two Miley airfoil models cast from the same mold. These smooth epoxy models each had a chord of 250 mm and a span of 421 mm. One model was used as a force model and for flow-visualization and hot-wire experiments. The other model was cast with 90 static pressure taps for pressure measurements.[8,9] The airfoil models were hung from the balance by a sting and "floated" between $9.5\times610\times610$ mm side plates.

Data Acquisition System

The data acquisition system used for these experiments is based on the Apple II Plus microcomputer. Auxiliary Apple brand components included a thermal printer, a video monitor, and minifloppy disk drives. In order to use the computer as an effective experimental aid, aftermarket devices were installed inside the Apple II computer. These devices are used to measure the voltage output of an instrument with analog-to-digital (A/D) conversion, or to drive a piece of equipment with digital-to-analog (D/A) conversion. An additional device with a telephone coupler allows the transfer of data between the microcomputer and the Notre Dame Computing Center IBM 3033 computer. In addition to the computer system with the data acquisition devices, a Scanivalve and electronic manometers with analog voltage outputs were used for pressure-measuring experiments. A pitot static tube was mounted in the wind tunnel test section in front of and above the airfoil model which had static pressure taps in its surface. Setra Systems digital readout electronic manometers (Models 339B and 339H) were used to measure the dynamic pressure from the pitot static tube and the pressure difference at each pressure tap. All data presented in the following sections are time-averaged data.

Results

A large amount of lift/drag flow measurements, flow-visualization and static pressure distributions, and hot-wire anemometer data were obtained for the Lissaman 7769 and/or the Miley M06-13-128 airfoil from $R_c=70{,}000$ to 600,000. The flow-visualization and/or pressure distributions help to explain the behavior of the airfoil boundary layer which produces the measured lift and drag characteristics, while the hot-wire anemometer data indicate the separation and transition locations and the character of the boundary layer.

Lift and drag coefficients were computed based on the corresponding freestream velocity measured at each angle of attack. The lift and drag coefficients were then corrected using

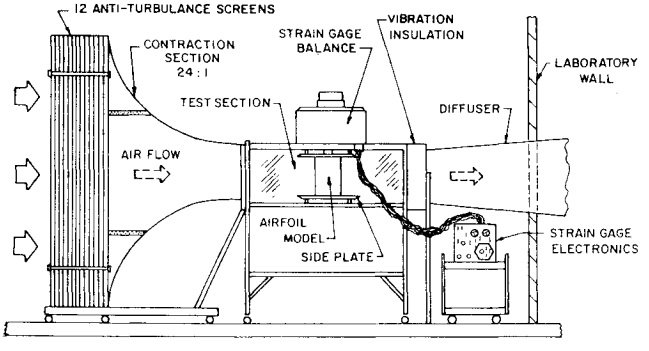

Fig. 4 Low-turbulence subsonic wind tunnel showing external strain-gage balance and side-plate arrangement.

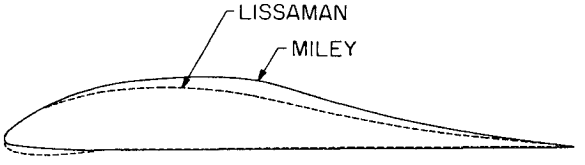

Fig. 5 Lissaman 7769 and Miley M06-13-128 airfoil geometries.

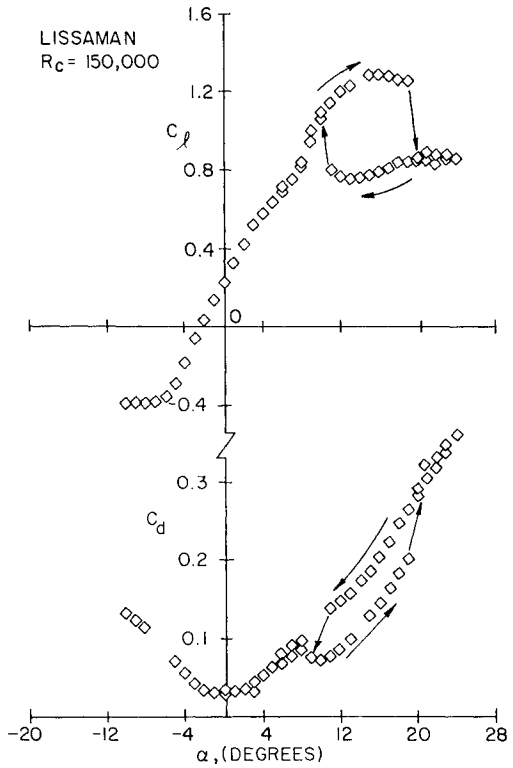

Fig. 6 Section lift and profile drag coefficients vs angle of attack for $R_c = 150{,}000$ for the smooth Lissaman airfoil (standard tunnel configuration).

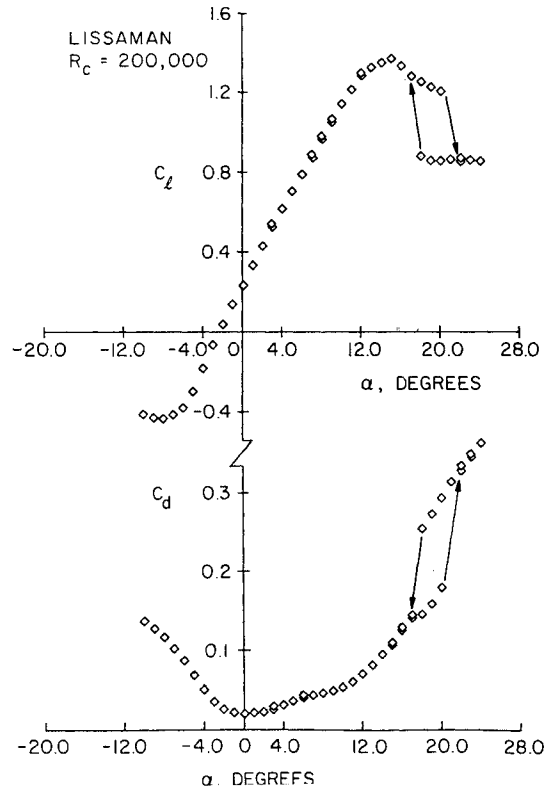

Fig. 7 Section lift and profile drag coefficients vs angle of attack for $R_c = 200{,}000$ for the smooth Lissaman airfoil (standard tunnel configuration).

the standard AGARD corrections for solid body blockage, wake blockage, streamline curvature, and buoyancy effects.[10]

Lissaman 7769 Airfoil

The lift and drag performance of the smooth (i.e., no strips of tape) Lissaman airfoil (Figs. 6-8) was obtained in the standard wind tunnel configuration (i.e., no turbulence screen or flow restrictor and freestream turbulence is less than 0.1%). Hysteresis is present for all of the Reynolds numbers studied. A detailed discussion of this airfoil and the influence of the disturbance environment will be presented for $R_c = 150{,}000$. Figure 9 illustrates the evolution of the flow at this Reynolds number as the airfoil angle of attack varies.† For angles from about 0 to 8 deg, the laminar boundary layer separates from the airfoil's upper surface. The resulting free shear layer appears to transition, however, there is no sign of reattachment taking place. This flow behavior causes the reduced lift curve slope and increased drag evident in Fig. 6. Between 10 and 20 deg, the flow is attached over much of the airfoil's upper surface with the result being an increase in the lift curve slope and a reduction in the drag's growth rate. Turbulent separation near the trailing edge, suggested by Figs. 9d and 9e and by the gentle rounding of the lift curve, is apparently responsible for the airfoil's stall. The abrupt loss in lift which occurs at about 20-deg angle of attack is the result of laminar separation near the leading edge. This sort of behavior usually indicates the bursting of a separation bubble. Therefore, the appearance of attached flow at 10 deg may be the product of the formation of a separation bubble. A reduction in angle of attack does not alter the separated flow pattern until 10 deg is reached. Thus, a high $C_{\ell\,\max}$ hysteresis is evident. Figures 9e and 9g show the flow patterns that characterize the two branches of the hysteresis loop. The presence and extent of this hysteresis were

†All data were taken while the airfoil was stationary whether the angle of attack was increased or decreased to obtain a given condition.

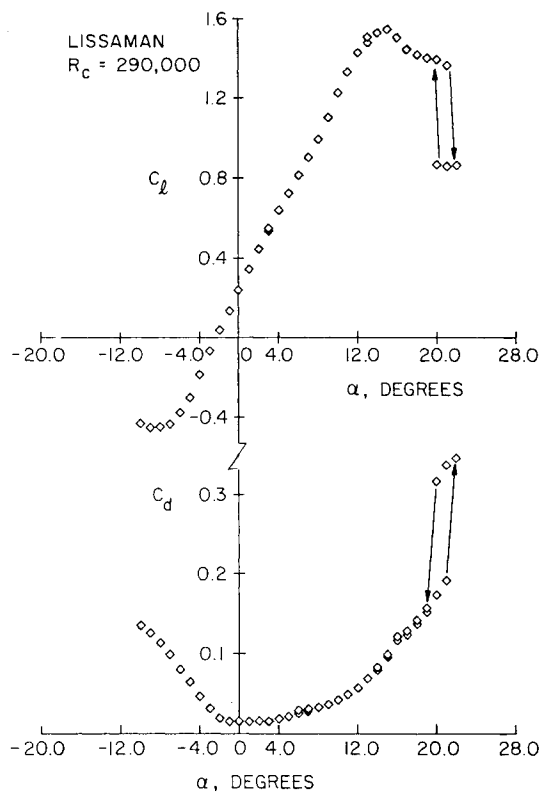

Fig. 8 Section lift and profile drag coefficients vs angle of attack for $R_c = 290{,}000$ for the smooth Lissaman airfoil (standard tunnel configuration).

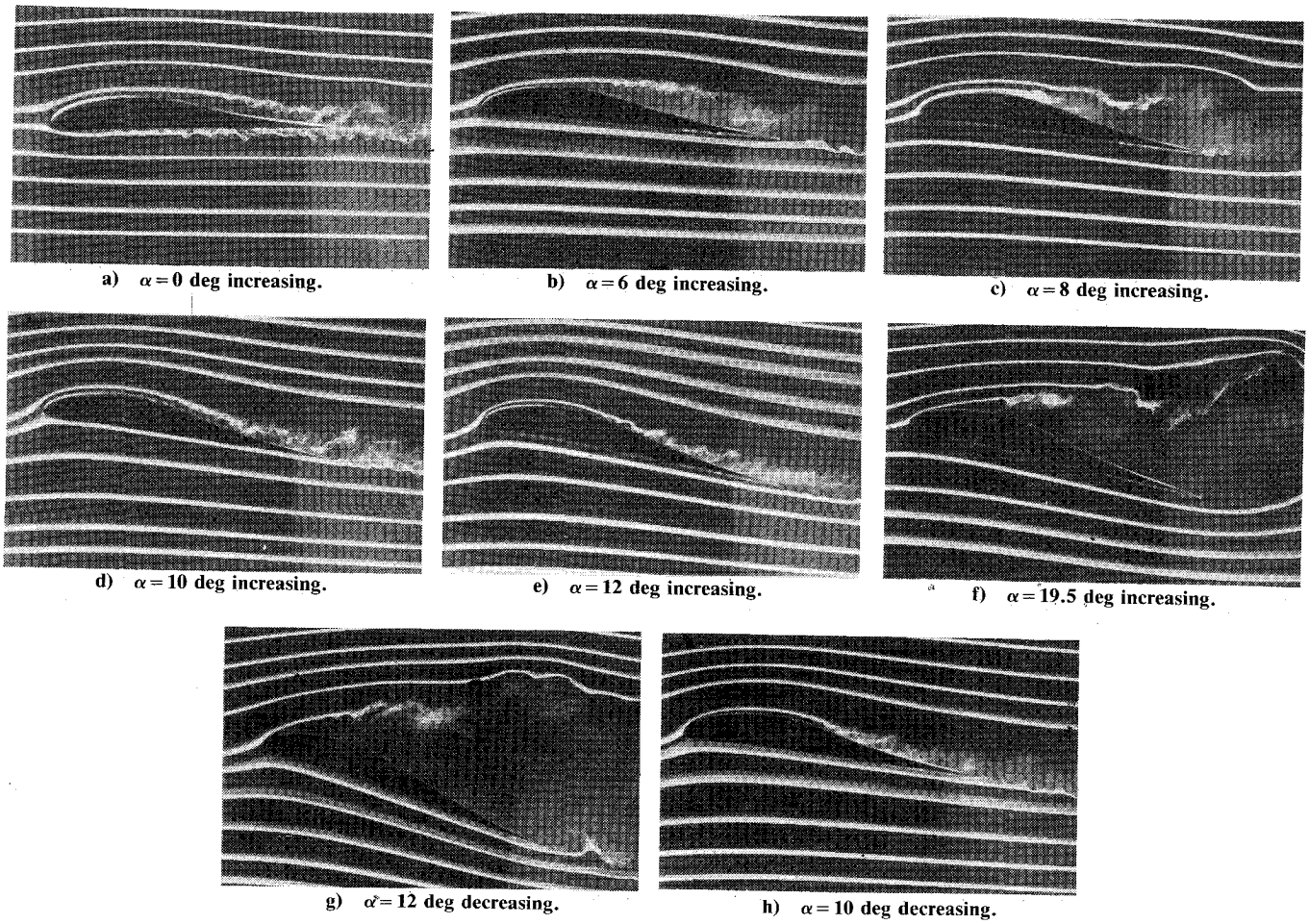

a) $\alpha = 0$ deg increasing. b) $\alpha = 6$ deg increasing. c) $\alpha = 8$ deg increasing.

d) $\alpha = 10$ deg increasing. e) $\alpha = 12$ deg increasing. f) $\alpha = 19.5$ deg increasing.

g) $\alpha = 12$ deg decreasing. h) $\alpha = 10$ deg decreasing.

Fig. 9 Smoke-visualization photographs of the smooth Lissaman airfoil at $R_c = 150{,}000$ (standard tunnel configuration).

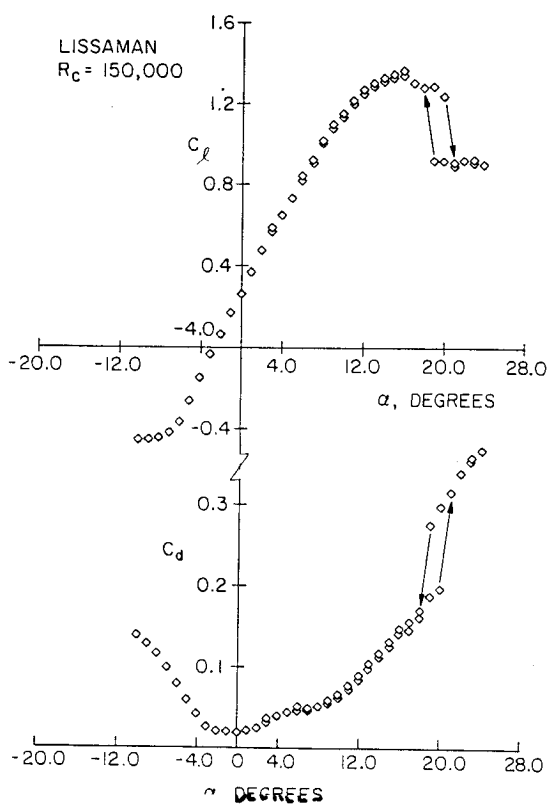

Fig. 10 Section lift and profile drag coefficients vs angle of attack for $R_c = 150{,}000$ for the smooth Lissaman airfoil (one flow restrictor and no screen).

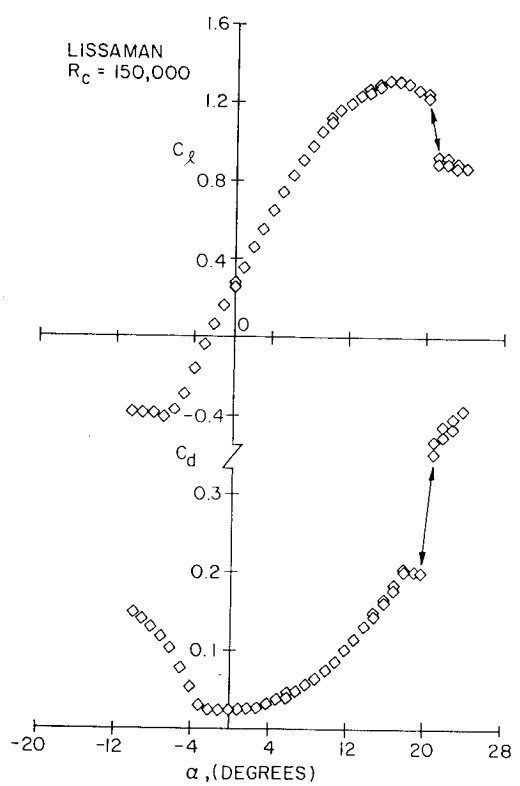

Fig. 11 Section lift and profile drag coefficients vs angle of attack for $R_c = 150{,}000$ for the smooth Lissaman airfoil (one 7.09-meshes/cm screen and no flow restrictor).

determined by the location of separation and transition in the boundary layer. The location of transition from laminar to turbulent flow in the boundary layer has long been known to be affected by the level and type of freestream disturbances and by the magnitude of the Reynolds number.

When the chord Reynolds number was increased to 200,000 (using the standard wind tunnel configuration), the hysteresis region was reduced (Fig. 7). At this condition the abrupt decrease in lift occurred at about 19 deg for increasing angle of attack and the lift jumped up when the angle of attack was decreased to 16 deg. At a chord Reynolds number of about 300,000 (Fig. 8), the abrupt decrease in lift occurred at about 21 deg and jumped back up at about 20 deg.

The result of changing the acoustical environment by adding one flow restrictor at the end of the test section is shown in Fig. 10. The addition of one restrictor increases both the freestream turbulence level and the sound pressure level since the fan speed must be increased for a fixed value of tunnel velocity. This test section environment reduced the size of the hysteresis region and produced a slightly higher $C_{\ell \max}$. A slightly lower minimum drag coefficient was also obtained. The use of two flow restrictors (i.e., still higher fan speed) produced similar results with the hysteresis being eliminated almost completely. Apparently the increase in freestream turbulence and acoustic excitation caused the laminar shear layer to transition much earlier, thus allowing the flow to reattach sooner.

Increasing the freestream turbulence level to about 0.3%, by adding one 7.09-meshes/cm screen at the upstream end of the test section with no flow restrictor, produced the lift and drag coefficients presented in Fig. 11. This test section environment completely eliminated the hysteresis region. With a larger turbulence intensity in the test section the airfoil boundary-layer transitions very close to the leading edge, eliminating hysteresis by enabling the flow to reattach at higher angles of attack.

Freestream disturbances are a major source of deviations in experimental data. However, there are other sources of disparity that produce results similar to those caused by freestream turbulence. The lift and drag curves produced in the standard wind tunnel environment with a strip of tape 2.55 mm wide and 0.15 mm thick placed near the leading edge (i.e., across the span at 1.1% chord) of the airfoil[8] are similar to the results shown in Fig. 10. This small boundary-layer trip reduced the hysteresis in a manner similar to the introduction of a flow restrictor. The tape produces similar results by causing early transition of the free shear layer. A model with a small amount of surface roughness or irregularities in the surface caused by fabrication defects could produce similar results.

Thus, although freestream disturbances produced the largest disparity between different tests for the Lissaman airfoil, not all of the differences can be attributed to freestream disturbances. Model imperfections or surface roughness can produce results identical to those achieved with freestream disturbances. Reynolds number effects are critical at low speeds. An increase in Reynolds number from 150,000 to 200,000 will eliminate a major portion of the hysteresis, and at 300,000 the hysteresis is insignificant. It is important that the freestream disturbances be well documented for each test condition in order to correctly attribute differences in test results to these freestream disturbances. A clear distinction between the effects of freestream disturbances, model irregularities, and Reynolds number must be made before the performance of airfoils at these Reynolds numbers can be understood.

Miley M06-13-128 Airfoil

Although experimental data were obtained for the Miley airfoil at chord Reynolds numbers from 70,000 to 600,000,[8,9] only the data obtained from $R_c = 100{,}000$ to 200,000 will be used in this discussion of hysteresis and the influence of the disturbance environment. Some results obtained using the strain-gage force balance and the microcomputer data acquisition system are shown in Figs. 12-14. The section lift coefficient and section profile drag coefficient vs angle of attack are presented in Figs. 12-14 for $R_c \simeq 100{,}000$, 150,000, and 200,000, respectively. The lift coefficient is zero at an angle of

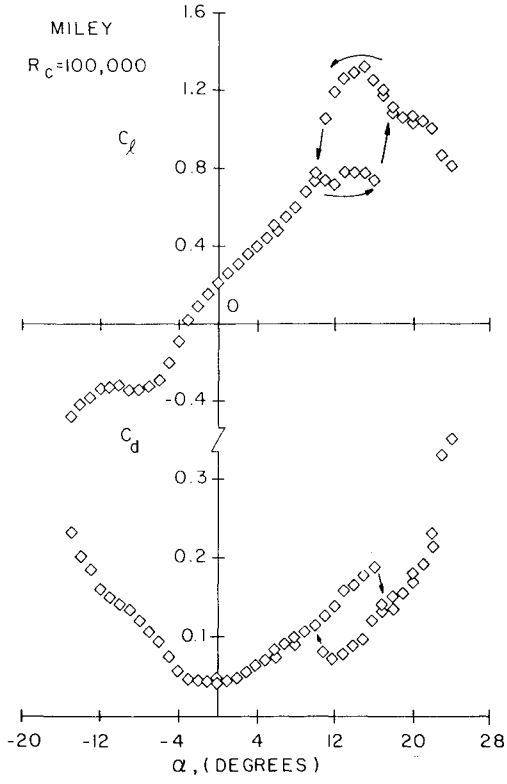

Fig. 12 Section lift and profile drag coefficients vs angle of attack for $R_c = 100{,}000$ for the smooth Miley airfoil (one flow restrictor and no screen).

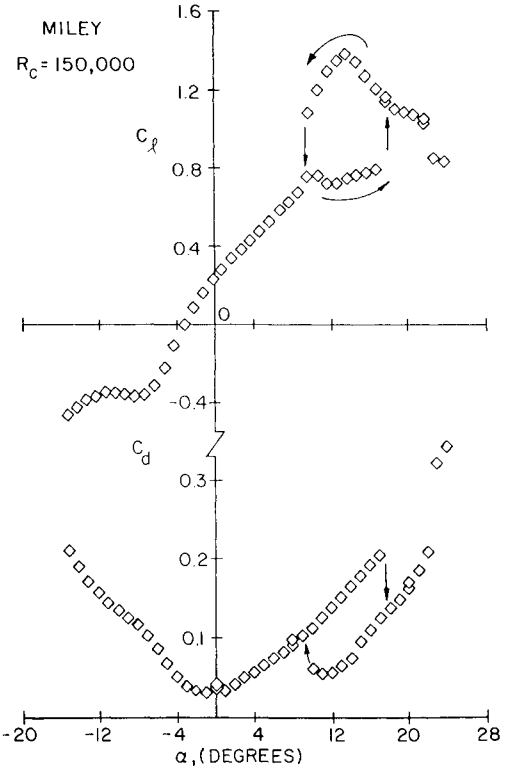

Fig. 13 Section lift and profile drag coefficients vs angle of attack for $R_c = 150{,}000$ for the smooth Miley airfoil (standard tunnel configuration).

attack of about −3 deg for all of the Reynolds numbers studied. At chord Reynolds numbers of 100,000 and 150,000 there is significant hysteresis in the lift and drag forces as shown in Figs. 12 and 13. The smoke-visualization photographs shown in Fig. 15 for $R_c \simeq 150{,}000$ are helpful in understanding how the hysteresis is produced in these experiments. At an angle of attack of zero (Fig. 15a), the boundary layer separates near the maximum thickness location on the upper surface, whereas the flow remains attached along the entire lower surface. There is no radical change in the observed behavior of the upper- and lower-surface boundary layers as the angle of attack increases to about 9 deg.

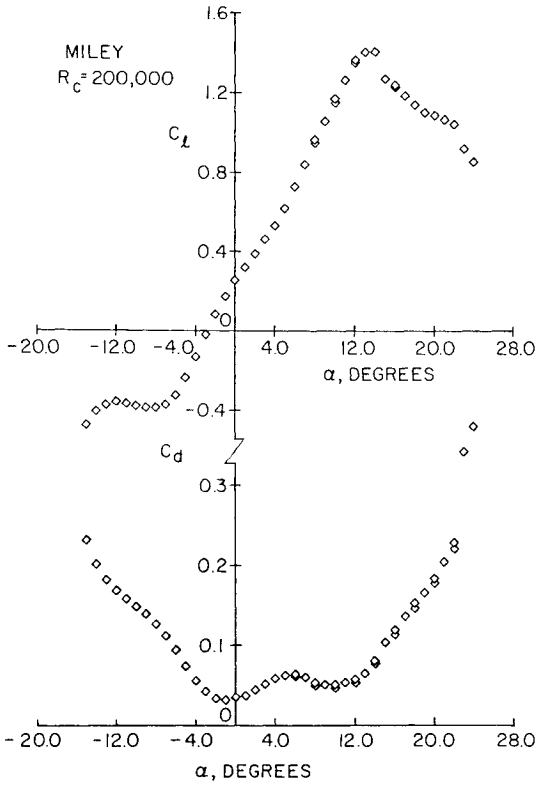

Fig. 14 Section lift and profile drag coefficients vs angle of attack for $R_c = 200{,}000$ for the smooth Miley airfoil (standard tunnel configuration).

However, there is some upstream movement of the separation point and the pressure distribution is altered to produce greater lift, etc.[9] Increasing the angle of attack to 13 deg (Fig. 15c), and then to 15 deg (Fig. 15d), moves the laminar separation point toward the leading edge with very little change in lift and a continuous increase in drag. At about 17 deg, the lift increases dramatically while the drag decreases. This behavior, similar to that of the Lissaman airfoil at an angle of attack of 10 deg, indicates that flow reattachment has occurred. After this jump the lift drops off gradually, while the drag increases as a result of a turbulent separated flow region which grows in extent with angle of attack. Decreasing the angle of attack from about 20 deg produces a much larger lift and lower drag from 17 to 10 deg than was measured for increasing angles. Thus, low $C_{\ell\,\max}$ hysteresis occurs because the airfoil boundary layer has an entirely different character when the angle of attack is increasing toward about 20 deg than when it is decreasing from about 20 deg.

At a chord Reynolds number of 200,000 and higher, no hysteresis is present and this smooth airfoil performs as expected. It is clear from these figures that operating the Miley airfoil, which was designed for $R_c \simeq 600{,}000$, at Reynolds numbers below 200,000 severely degrades its performance and produces a hysteresis loop that acts in the opposite sense as the loop produced by the Lissaman airfoil.

Although the hysteresis loop for $R_c = 100{,}000$ was documented and verified with static pressure measurements,[8,9] the surface roughness due to the very small static pressure taps in the pressure model was enough to eliminate hysteresis at $R_c \simeq 150{,}000$. For this reason the influence of the disturbance environment was also studied for the Miley airfoil at this Reynolds number. The addition of one flow restrictor increased the freestream turbulence level from 0.07 to 0.16%, while the introduction of one 7.09-meshes/cm screen upstream of the model raised the freestream turbulence level from 0.07 to about 0.30%. A strip of tape 0.127 mm thick and 2.21 mm wide was placed on the airfoil with the leading edge of the tape at 0.013c. The results indicated that the hysteresis loop was eliminated for all three cases. Although laminar separation occurs without reattachment for increasing angle of attack on the Miley airfoil producing a hysteresis loop of the opposite sense as the one found with the Lissaman, this hysteresis was eliminated by any increase in the disturbance environment at $R_c \simeq 150{,}000$ or increase in the chord Reynolds number above a value of about 150,000.

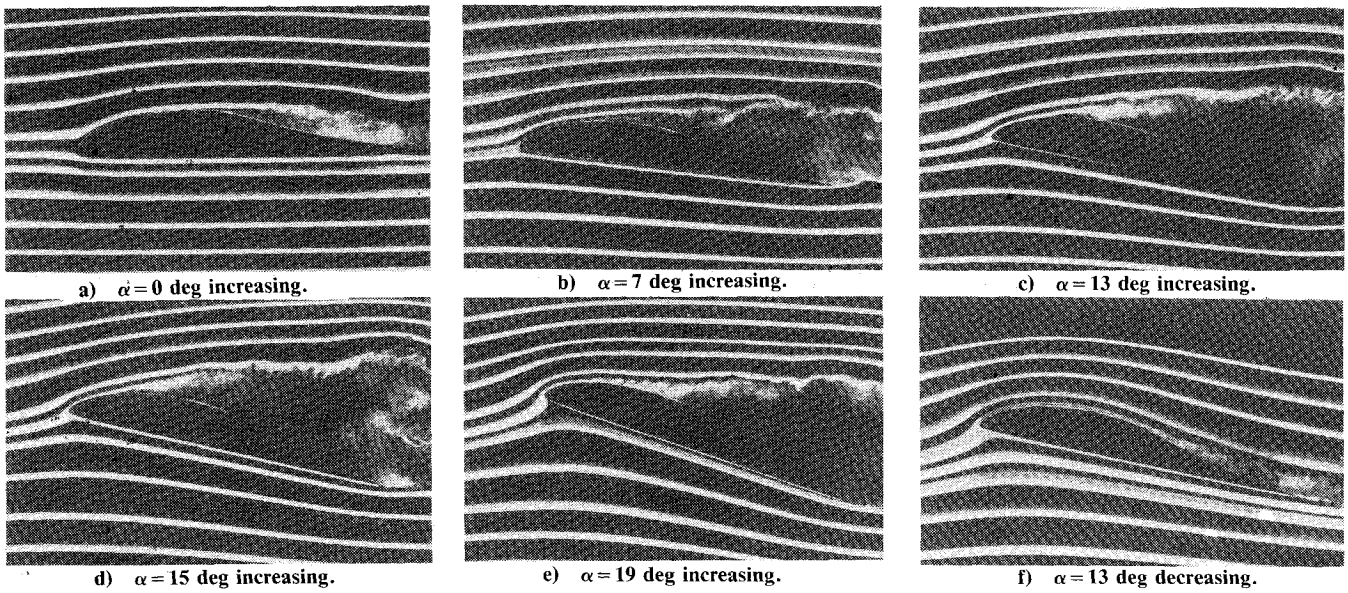

a) $\alpha = 0$ deg increasing. b) $\alpha = 7$ deg increasing. c) $\alpha = 13$ deg increasing.

d) $\alpha = 15$ deg increasing. e) $\alpha = 19$ deg increasing. f) $\alpha = 13$ deg decreasing.

Fig. 15 Smoke-visualization photographs of the smooth Miley airfoil at $R_c = 150{,}000$ (standard tunnel configuration).

Concluding Remarks

For both the Lissaman and Miley airfoils, one branch of the hysteresis loop consists of a separated laminar boundary layer, the other of attached flow over much of the airfoil. The attached flow branch appears to be the result of the laminar free shear layer transitioning and reattaching as a turbulent boundary layer. In other words, a separation bubble is the mechanism for obtaining attached flow on these airfoils at low Reynolds numbers.

At low angles of attack both airfoils experience laminar separation. Reattachment takes place on the Lissaman airfoil at moderate angles of attack. However, this is not the case for the Miley airfoil section. This means that its free shear layer is not transitioning within a sufficiently short distance for the turbulent mixing process to cause reattachment. At high angles of attack the Lissaman separation bubble "bursts," which results in the reappearance of separated laminar flow. This corresponds to the onset of a high $C_{\ell \max}$ hysteresis. On the other hand, the Miley airfoil finally undergoes flow reattachment at large angles of attack. Downstream of reattachment, however, large-scale separation of the turbulent boundary layer appears to dominate the force characteristics. For this reason, further increases in incidence do not reveal the abrupt loss in lift and increase in drag (i.e., the onset of high $C_{\ell \max}$ hysteresis) seen in connection with the Lissaman airfoil. Instead, by reducing the angle of attack, the extent of the turbulent separated region is diminished and the force characteristics improve. Thus, a low $C_{\ell \max}$ hysteresis appears.

Therefore, for the Miley airfoil, inability of the laminar free shear layer to reattach until angles of attack are reached where turbulent separation occurs is responsible for the Miley's low $C_{\ell \max}$ hysteresis. Increasing the Reynolds number or freestream disturbance level results in earlier transition and reattachment of the free shear layer. However, the dominance of turbulent separated flow at high angles of attack still eliminates the occurrence of the kind of hysteresis encountered by the Lissaman profile. Thus, the shape of an airfoil, which controls boundary-layer separation, is also an important factor in the type of hysteresis that occurs or whether it will appear at all.

The problems associated with obtaining accurate wind tunnel data for airfoil sections at low Reynolds numbers are compounded by the extreme sensitivity of the boundary layers to the freestream disturbance environment. The effect of freestream disturbances varies with magnitude, frequency content, and source of the disturbance. Further research especially concerning the effect of frequency content and the possible coupling of acoustic and velocity fluctuations is necessary. The sensitivity and accuracy of the measurement and data acquisition systems, as well as the experimental procedure used, can have a substantial effect on the results obtained.

Acknowledgments

This research was supported by NASA Langley Research Center under Grant NSG-1419, the Naval Research Laboratory under Contract N00014-81-K-2036, and by the Office of Naval Research under Contract N00014-83-K-0239. It is a pleasure to thank L. J. Pohlen, P. E. Conigliaro, and B. J. Jansen Jr. for their dedication in obtaining most of the data used in this paper. Sincere thanks also go to colleagues at the University of Notre Dame, T. J. Akai and S. M. Batill, and our current graduate students, M. Brendel, A. F. Huber II, W. G. Bastedo Jr., and M. M. O'Meara, and especially G. S. Schmidt, for their comments and suggestions during the writing of this paper.

References

[1]Schmitz, F. W., "Aerodynamics of the Model Airplane, Part I, Airfoil Measurements," NASA-TM-X-60976, 1967.

[2]Mueller, T. J. and Batill, S. M., "Experimental Studies of Separation on a Two-Dimensional Airfoil at Low Reynolds Numbers," *AIAA Journal*, Vol. 20, April 1982, pp. 457-463.

[3]Mueller, T. J. and Jansen, B. J. Jr., "Aerodynamic Measurements at Low Reynolds Numbers," AIAA Paper 82-0598, March 1982.

[4]Miley, S. J., "An Analysis of the Design of Airfoil Sections for Low Reynolds Numbers," Ph.D. Dissertation, Mississippi State University, Jan. 1972.

[5]Mueller, T. J., Pohlen, L. J., Conigliaro, P. E., and Jansen, B. J. Jr., "The Influence of Free-Stream Disturbances on Low Reynolds Number Airfoil Experiments," *Experiments in Fluids*, Vol. 1, 1983, pp. 3-14.

[6]Mueller, T. J., "Flow Visualization by Direct Injection," *Fluid Mechanics Measurements*, edited by R. J. Goldstein, Hemisphere Publishing Corp., Washington, D. C., 1983, Chap. 7, pp. 307-375.

[7]Burke, J. D., "The Gossamer Condor and Albatross: A Case Study in Aircraft Design," AIAA Professional Study Series, Rept. AV-R80/540, 1980.

[8]Pohlen, L. J., "Experimental Studies of the Effect of Boundary Layer Transition on the Performance of the Miley (M06-13-128) Airfoil at Low Reynolds Numbers," M.S. Thesis, University of Notre Dame, IN, Jan. 1983.

[9]Pohlen, L. J. and Mueller, T. J., "Boundary Layer Characteristics of the Miley Airfoil at Low Reynolds Numbers," *Journal of Aircraft*, Vol. 21, Sept. 1984, pp. 658-664.

[10]Rogers, E. W. E., "Blockage Effects in Closed or Open Tunnels," AGARDOgraph 109, 1966, pp. 279-340.